Weierstraß-Institut
für Angewandte Analysis und Stochastik
Leibniz-Institut im Forschungsverbund Berlin e. V.

Preprint ISSN 0946 – 8633

On the probability density function of baskets

Christian Bayer[1], Peter K. Friz[1,2], Peter Laurence[3]

submitted: June 12, 2013

[1] Weierstrass Institute
Mohrenstr. 39
10117 Berlin
Germany
E-Mail: christian.bayer@wias-berlin.de
peter.friz@wias-berlin.de

[2] Institute of Mathematics
TU Berlin
Strasse des 17. Juni 136
10623 Berlin
Germany
E-Mail: friz@math.tu-berlin.de

[3] Università di Roma
Piazzale Aldo Moro 5
00185 Rome
Italy
E-Mail: laurencepm@yahoo.com

No. 1796
Berlin 2013

2010 *Mathematics Subject Classification.* 91G20, 60F10, 65C50.

Key words and phrases. Sums of lognormals, focality, pricing of butterfly spreads on baskets.

Edited by
Weierstraß-Institut für Angewandte Analysis und Stochastik (WIAS)
Leibniz-Institut im Forschungsverbund Berlin e. V.
Mohrenstraße 39
10117 Berlin
Germany

Fax: +49 30 20372-303
E-Mail: preprint@wias-berlin.de
World Wide Web: http://www.wias-berlin.de/

Abstract

The state price density of a basket, even under uncorrelated Black–Scholes dynamics, does not allow for a closed from density. (This may be rephrased as statement on the sum of lognormals and is especially annoying for such are used most frequently in Financial and Actuarial Mathematics.) In this note we discuss short time and small volatility expansions, respectively. The method works for general multi-factor models with correlations and leads to the analysis of a system of ordinary (Hamiltonian) differential equations. Surprisingly perhaps, even in two asset Black–Scholes situation (with its flat geometry), the expansion can degenerate at a critical (basket) strike level; a phenomena which seems to have gone unnoticed in the literature to date. Explicit computations relate this to a phase transition from a unique to more than one "most-likely" paths (along which the diffusion, if suitably conditioned, concentrates in the afore-mentioned regimes). This also provides a (quantifiable) understanding of how precisely a presently out-of-money basket option may still end up in-the-money.

1 Introduction

As is well known, the sum of independent log-normal variable does not admit a closed-form density. And yet, there are countless applications in Finance and Actuarial Mathematics where such sums play a crucial role, consider for instance the law of a Black–Scholes basket B at time T, i.e. the weighted average of d geometric Brownian motions.

As a consequence, there is a natural interest in approximations and expansions, see e.g. [14] and the references therein. This article contains a detailed investigation in small volatility and short time regimes. Forthcoming work of A. Gulisashvili and P. Tankov deals with tail asymptotics. Our methods are not restricted to the geometric Brownian motion case: in principle, each Black–Scholes component could be replaced by the asset price in a stochastic volatility model, such as the the Stein–Stein model [37], with full correlation between all assets and their volatilities. In the end, explicit solutions only depend on the analytical tractability of a system of ordinary differential equations. If such tractability is not given, one can still proceed with numerical ODE solvers.

As a matter of fact, our aim here is no too push the generality in which our methods work: one can and should expect involved answers in complicated models. Rather, our main – and somewhat surprising – insight is that *unexpected phenomena* are already present in the *simplest possible setting*: to this end, our first focus will be on the case of $d = 2$ independent Black–Scholes assets, without drift and correlation, with unit spot and unit volatility). To be more specific, if C_B denotes the fair value of an (out-of-money) call option on the basket B struck at K, one naturally expects, for a small maturity T,

$$\frac{\partial^2}{\partial K^2} C_B(K,T) \sim (\text{const}) \exp\left(-\frac{\Lambda(K)}{T}\right) \frac{1}{\sqrt{T}}.$$

And yet, while true for *most* strikes, it fails for $K = K^*$; in fact,

$$\left\{\frac{\partial^2}{\partial K^2} C_B(K,T)\right\}_{K=K^*} \sim (\text{const}) \exp\left(-\frac{\Lambda(K^*)}{T}\right) \frac{1}{T^{3/4}}.$$

To the best of our knowledge, and despite the seeming triviality of the situation (two independent Black–Scholes assets!), the existence of a "special" strike level K^*, at which the value of a basket option (here: butterfly spread[1]) has a "special" decay behavior, as maturity approaches, seems to be new. There are different proofs of this fact; the most elementary argument – based on the analysis of a convolution integral – is given in Section 2. However, this approach – while telling us *what* happens – does not tell us *how* it happens.

The main contribution of this note is precisely a good understanding of the latter. In fact, there is clear picture that comes with K^*. For $K < K^*$, and conditional on the option to expire on the money, there is a unique "most likely" path around which the underlying asset price process will concentrate as maturity approaches. For $K > K^*$, however, this ceases to be true: there will be two distinct (here: equally likely) paths around which concentration occurs. What underlies this interpretation is that large deviation theory, which on a deep level underlies our methods, not only characterizes the probability of unlikely events (such as expiration in-the-money, if presently out-of-the-money, as time to maturity goes to zero) but also the mechanism via which these events can occur. Such understanding was already crucial in previous works on baskets, starting with [1, 2], aiming at quantification of basket (implied vol) skew relative to its components. As a matter of fact, the analysis in these paper relied on the statement that "generically there is a unique arrival point [of a unique energy minimizing path] on the (basket-strike) arrival manifold". The situation, however, even in the Black–Scholes model, is more involved. And indeed, we shall establish existence of a critical strike K^*, at which one sees the phase-transition from one to two energy minimizing, "most likely", paths.[2] And this information will have meaning to traders (as long as they believe in a diffusion model as maturity approaches, which may or may not be a good idea ...) as it tells them the possible scenarios in which an out-of-the money basket option may still expire in the money.

Let us conclude this introduction with a few technical notes. We view the evolution of the basket price – even in the Black-Scholes model – as a stochastic volatility evolution model; by which we mean $dB_t/B_t = \sigma(t,\omega)dW_t$ (as opposed to a local vol evolution where $\sigma = \sigma(t, B_t)$). This should explain why the methods developed in Part I of [10, 11] for the analysis of stochastic volatility models (then used in Part II, [11], to solve the concrete smile problem (shape of the wings) for the correlated Stein–Stein model), are also adequate for the analysis of baskets. In a sense, the present note may well be viewed as Part III in this sequence of papers.

Acknowledgment: P.K.F. has received partial funding from the European Research Council under the European Union's Seventh Framework Program (FP7/2007-2013) / ERC grant agreement nr. 258237.

[1] Extensions to spreads and vanilla options are possible and will be discussed elsewhere.

[2] It can be shown that, sufficiently close to the arrival manifold, there is in fact a unique energy minimizing paths. The (near-the-money) analysis of [1, 2] is then justified.

2 Computations based on saddle-point method

In terms of a standard d-dimensional Wiener process $\left(W^1, \ldots, W^d\right)$,

$$B_T = \sum_{i=1}^{d} S_0^i \exp\left(\mu^i T + \sigma^i W_T^i\right).$$

Write $f = f_T(K)$ for the probability density function of B_T; i.e. for $\mathbb{P}[B_T \in [K, K + dK]]/dK$. Of course, it is given by some $(d-1)$-dimensional convolution integral, explicit asymptotic expansions are - in principle - possible with the saddle point method. It will be enough for our purposes to illustrate the method in the afore-mentioned simplest possible setting:

$$d = 2,\ S_0^1 = S_0^2 = 1,\ \mu^1 = \mu^2 = 0,\ \sigma^1 = \sigma^2 = 1.$$

In other words $B_T = \exp\left(W_T^1\right) + \exp\left(W_T^2\right)$; we claim that

$$f(K) = \begin{cases} \exp\left(-\dfrac{\Lambda(K)}{T}\right)\dfrac{1}{\sqrt{T}}\left(1 + O(T)\right) & \text{when } K \neq K^* \quad (1a) \\ \exp\left(-\dfrac{\Lambda(K^*)}{T}\right)\dfrac{1}{T^{3/4}}\left(1 + O(T)\right) & \text{when } K = K^* \quad (1b) \end{cases}$$

with

$$K^* = 2e \approx 5.43656$$

and

$$\Lambda(K) = \log(K/2)^2.$$

With the minimal $x^* = K/2$ as established below we immediately have $f(K) \approx exp(-h_K(x^*)/(2T))$ and since $h_K(x^*) \sim 2(logK/2)^2 asT \to 0$, we get $\Lambda(K)$ as given above. Here, we are interested in establishing the two regimes proposed in (1). The stock price S_T^i has a log-normal distribution with parameters $\mu^i = \log(S_0^i) - \frac{(\sigma^i)^2 T}{2} = -T/2$ and $\xi^i = \sigma^i\sqrt{T} = \sqrt{T}$, where the density of the log-normal distribution is given by

$$f_{\mu,\xi}(x) = \frac{1}{\sqrt{2\pi}\xi x}\exp\left(-\frac{(\log x - \mu)^2}{2\xi^2}\right). \quad (2)$$

Obviously, the density of the sum of these two independent log-normal random variables satisfies

$$f(K) = \int_0^K f_{\mu^1,\xi^1}(K - x) f_{\mu^2,\xi^2}(x)dx. \quad (3)$$

Using our special parameters, the integrand is of the form

$$f_{\mu^1,\xi^1}(K - x) f_{\mu^2,\xi^2}(x) = \frac{1}{2\pi T x(K - x)}\exp\left(-\frac{h_K(x)}{2T}\right)$$

with

$$h_K(x) := \left(\log x + \frac{T}{2}\right)^2 + \left(\log(K - x) + \frac{T}{2}\right)^2. \quad (4)$$

In order to apply the Laplace approximation to (3), we compute the minimizer for h_K, which is found by the first order condition

$$h_K'(x) = 0 \iff \frac{\log x + T/2}{x} - \frac{\log(K-x) + T/2}{K-x} = 0.$$

Clearly, this equation is solved by choosing $x^* = K/2$. Now let us check degeneracy of that minimum by computing

$$h_K''(x^*) = h_K''(K/2) = 16\frac{1 - \log(K/2) - T/2}{K^2}.$$

Thus, we find that

$$h_K''(x^*) = 0 \iff K = 2e^{1-T/2} \sim 2e, \text{ for } T \to 0. \tag{5}$$

Choosing $K = 2e^{1-T/2}$ and, correspondingly, $x^* = e^{1-T/2}$, we obtain the Taylor expansion $h_K(x) = h_K(x^*) + \frac{h_K^{(4)}(x^*)}{24}(x-x^*)^4 + O((x-x^*)^5)$, with $h_K(x^*) = 2$ and $h_K^{(4)}(x^*) = 20e^{2T-4}$, we obtain the Laplace approximation

$$\begin{aligned} f(K) &= \int_0^K \frac{1}{2\pi T(K-x)x} \exp\left(-\frac{h_K(x)}{2\pi}\right) dx \\ &= \frac{1}{2\pi T e^{2-T}} \int_0^K \exp\left(-\frac{1}{T}\right) \exp\left(-\frac{5e^{2T-4}(x-K/2)^4}{12T}\right) dx\,(1+O(T)) \\ &= \frac{3^{1/4}\Gamma(1/4)}{5^{1/4} 2\sqrt{2}\pi e} \exp\left(-\frac{1}{T}\right) \frac{1}{T^{3/4}}\,(1+O(T)), \end{aligned}$$

where we used

$$\int_{-\infty}^{\infty} \exp(-\alpha x^4) dx = \frac{\Gamma(1/4)}{2\alpha^{1/4}}, \quad \alpha > 0.$$

Thus, we arrive at (1).

3 Large Deviations approach

Our main tool here are novel marginal density expansions in small-noise regime [10]. This was used in order to compute the large-strike behavior of implied volatility in the correlated Stein–Stein model; [37, 22].[3]

In fact, the technical assumptions of [10] were satisfied in the analysis of the Stein–Stein model whereas in the (seemingly) trivial case of two IID Black-Scholes assets, the technical assumptions of [10] are indeed violated for a critical strike $K = K^*$. The necessity of this condition is then highlighted by the fact, as was seen in the previous section,

$$\left\{\frac{\partial^2}{\partial K^2} C_B(K,T)\right\}_{K=K^*} \asymp (\text{const}) \exp\left(-\frac{\Lambda(K^*)}{T}\right) \frac{1}{T^{1/2}}$$

The computation of K^* can be achieved either via a geometric construction borrowed from Riemannian geometry, which relies on the Weingarten map, or by some (fairly) elementary analysis of a system of Hamiltonian ODEs. In fact, the Hamiltonian point of view extends

[3] Similar investigations have recently been conducted in the Heston model; [25, 21] and the references therein.

naturally when one introduces correlation, local and even stochastic volatility. Explicit answers then depend on the analytical tractability of these (boundary value) ODE problems. (Of course, the numerical solution of such problems is well-known.)

In the following, we review [10]. Consider a d-dimensional diffusion $(\mathrm{X}_t^\varepsilon)_{t\geq 0}$ given by the stochastic differential equation

$$d\mathrm{X}_t^\varepsilon = b\left(\varepsilon, \mathrm{X}_t^\varepsilon\right) dt + \varepsilon\sigma\left(\mathrm{X}_t^\varepsilon\right) dW_t, \quad \text{with } \mathrm{X}_0^\varepsilon = \mathrm{x}_0^\varepsilon \in \mathbb{R}^d \tag{6}$$

and where $W = (W^1, \ldots, W^m)$ is an m-dimensional Brownian motion. Unless otherwise stated, we assume $b : [0,1) \times \mathbb{R}^d \to \mathbb{R}^d$, $\sigma = (\sigma_1, \ldots, \sigma_m) : \mathbb{R}^d \to \mathrm{Lin}\left(\mathbb{R}^m, \mathbb{R}^d\right)$ and $\mathrm{x}_0^\cdot : [0,1) \to \mathbb{R}^d$ to be smooth, bounded with bounded derivatives of all orders. Set $\sigma_0 = b(0,\cdot)$ and assume that, for every multiindex α, the drift vector fields $b(\varepsilon,\cdot)$ converges to σ_0 in the sense[4]

$$\partial_x^\alpha b(\varepsilon,\cdot) \to \partial_x^\alpha b(0,\cdot) = \partial_x^\alpha \sigma_0(\cdot) \text{ uniformly on compacts as } \varepsilon \downarrow 0. \tag{7}$$

We shall also assume that

$$\partial_\varepsilon b(\varepsilon,\cdot) \to \partial_\varepsilon b(0,\cdot) \text{ uniformly on compacts as } \varepsilon \downarrow 0 \tag{8}$$

and

$$\mathrm{x}_0^\varepsilon = \mathrm{x}_0 + \varepsilon\hat{\mathrm{x}}_0 + o(\varepsilon) \text{ as } \varepsilon \downarrow 0. \tag{9}$$

Theorem 1. ***(Small noise)*** *Let (X^ε) be the solution process to*

$$d\mathrm{X}_t^\varepsilon = b\left(\varepsilon, \mathrm{X}_t^\varepsilon\right) dt + \varepsilon\sigma\left(\mathrm{X}_t^\varepsilon\right) dW_t, \quad \textit{with } \mathrm{X}_0^\varepsilon = \mathrm{x}_0^\varepsilon \in \mathbb{R}^d.$$

Assume $b(\varepsilon,\cdot) \to \sigma_0(\cdot)$ in the sense of (7), (8), and $\mathrm{X}_0^\varepsilon \equiv \mathrm{x}_0^\varepsilon \to \mathrm{x}_0$ as $\varepsilon \to 0$ in the sense of (9). Assume non-degeneracy of σ in the sense that $\sigma.\sigma^T$ is strictly positive definite everywhere in space. [5] *Fix $\mathrm{y} \in \mathbb{R}^l$, $N_\mathrm{y} := (\mathrm{y},\cdot)$ and let $\mathcal{K}_\mathrm{y}$ be the the space of all $\mathrm{h} \in H$, the Cameron-Martin space of absolutely continuous paths with derivatives in $L^2([0,T],\mathbb{R}^m)$, s.t. the solution to*

$$d\phi_t^\mathrm{h} = \sigma_0\left(\phi_t^\mathrm{h}\right) dt + \sum_{i=1}^m \sigma_i\left(\phi_t^\mathrm{h}\right) d\mathrm{h}_t^i, \ \phi_0^\mathrm{h} = \mathrm{x}_0 \in \mathbb{R}^d$$

satisfies $\phi_T^\mathrm{h} \in N_\mathrm{y}$. In a neighborhood of y, assume smoothness of[6]

$$\Lambda(\mathrm{y}) = \inf\left\{\frac{1}{2}||\mathrm{h}||_H^2 : \mathrm{h} \in \mathcal{K}_\mathrm{y}\right\}.$$

Assume also (i) there are only finitely many minimizers, i.e. $\mathcal{K}_\mathrm{y}^{\min} < \infty$ where

$$\mathcal{K}_\mathrm{y}^{\min} := \left\{\mathrm{h}_0 \in \mathcal{K}_\mathrm{y} : \frac{1}{2}||\mathrm{h}_0||_H^2 = \Lambda(\mathrm{y})\right\};$$

[4] If (6) is understood in Stratonovich sense, so that dW is replaced by $\circ dW$, the drift vector field $b(\varepsilon,\cdot)$ is changed to $\tilde{b}(\varepsilon,\cdot) = b(\varepsilon,\cdot) - \left(\varepsilon^2/2\right)\sum_{i=1}^m \sigma_i \cdot \partial\sigma_i$. In particular, σ_0 is also the limit of $\tilde{b}(\varepsilon,\cdot)$ in the sense of (7) .

[5] This may be relaxed to a weak Hoermander condition with an explicit controllability condition.

[6] If $\#\mathcal{K}_\mathrm{y}^{\min} = 1$ smoothness of the energy can be shown and need not be assumed; [10]. Note also that in our application to tail asymptotics, with θ-scaling, $\theta \in \{1,2\}$, the energy must be linear resp. quadratic (by scaling) and hence smooth.

(ii) x_0 *is non-focal for* N_{y} *in the sense of [10]. (We shall review below how to check this.) Then, for fixed* x_0, y *and* $T > 0$ *there exists* $c_0 = c_0(\mathrm{x}_0, \mathrm{y}, T) > 0$ *such that*

$$\mathrm{Y}_T^\varepsilon = \Pi_l \mathrm{X}_T^\varepsilon = \left(X_T^{\varepsilon,1}, \ldots, X_T^{\varepsilon,l}\right), \quad 1 \le l \le d$$

admits a density with expansion

$$f_\varepsilon(\mathrm{y}, T) = e^{-\frac{\Lambda(\mathrm{y})}{\varepsilon^2}} e^{\frac{\max\left\{\Lambda'(\mathrm{y})\cdot \hat{\mathrm{Y}}_T(\mathrm{h}_0) : \mathrm{h}_0 \in \mathcal{K}_{\mathrm{y}}^{\min}\right\}}{\varepsilon}} \varepsilon^{-l} (c_0 + O(\varepsilon)) \text{ as } \varepsilon \downarrow 0,$$

where Λ' *denotes the gradient of* Λ.

Here $\hat{\mathrm{Y}} = \hat{\mathrm{Y}}(\mathrm{h}_0) = \left(\hat{Y}^1, \ldots, \hat{Y}^l\right)$ *is the projection,* $\hat{\mathrm{Y}} = \Pi_l \hat{\mathrm{X}}$, *of the solution to the following (ordinary) differential equation*

$$\begin{aligned} d\hat{\mathrm{X}}_t &= \left(\partial_x b\left(0, \phi_t^{\mathrm{h}_0}(\mathrm{x}_0)\right) + \partial_x \sigma(\phi_t^{\mathrm{h}_0}(\mathrm{x}_0))\dot{\mathrm{h}}_0(t)\right)\hat{\mathrm{X}}_t dt + \partial_\varepsilon b\left(0, \phi_t^{\mathrm{h}_0}(\mathrm{x}_0)\right) dt, \qquad (10) \\ \hat{\mathrm{X}}_0 &= \hat{\mathrm{x}}_0. \end{aligned}$$

Remark 2 (Localization). The assumptions on the coefficients b, σ in theorem 1 (smooth, bounded with bounded derivatives of all orders) are typical in this context (cf. Ben Arous [5, 6] for instance) but rarely met in practical examples from finance. This difficulty can be resolved by a suitable localization. For instance, as detailed in [10], an estimate of the form

$$\lim_{R\to\infty} \limsup_{\varepsilon\to 0} \varepsilon^2 \log \mathbb{P}[\tau_R \le T] = -\infty. \qquad (11)$$

with $\tau_R := \inf\left\{t \in [0,T] : \sup_{s\in[0,t]} \left|\mathrm{X}_s^\varepsilon\right| \ge R\right\}$ will allow to bypass the boundedness assumptions.

3.1 Short time asymptotics

The reduction of *short time expansions* to small noise expansions by Brownian scaling is classical. In the present context, we have the following statement, taken from [10, Sec. 2.1].

Corollary 3. ***(Short time)*** *Consider* $d\mathrm{X}_t = b(\mathrm{X}_t)\,dt + \sigma(\mathrm{X}_t)\,dW$, *started at* $\mathrm{X}_0 = \mathrm{x}_0 \in \mathbb{R}^d$, *with* C^∞*-bounded vector fields which are non-degenerate in the sense that* $\sigma.\sigma^T$ *is strictly positive definite everywhere in space. Fix* $\mathrm{y} \in \mathbb{R}^l$, $N_{\mathrm{y}} := (\mathrm{y}, \cdot)$ *and assume (i),(ii)as in theorem 1. Let* $f(t,\cdot) = f(t,\mathrm{y})$ *be the density of* $\mathrm{Y}_t = \left(\mathrm{X}_t^1, \ldots, \mathrm{X}_t^l\right)$. *Then*

$$f(t,\mathrm{y}) \sim (const)\frac{1}{t^{l/2}} \exp\left(-\frac{d^2(\mathrm{x}_0, \mathrm{y})}{2t}\right) \text{ as } t \downarrow 0$$

where $d(\mathrm{x}_0, \mathrm{y})$ *is the sub-Riemannian distance, based on* $(\sigma_1, \ldots, \sigma_m)$, *from the point* x_0 *to the affine subspace* N_{y}.

3.2 Computational aspects

We present here the *mechanics* of the actual computations, in the spirit of the Pontryagin maximum principle (e.g. [36]). For details we refer to [10].

- **The Hamiltonian.** Based on the SDE (6), with diffusion vector fields $\sigma_1, \ldots, \sigma_m$ and drift vector field σ_0 (in the $\varepsilon \to 0$ limit) we define the *Hamiltonian*

$$\begin{aligned}\mathcal{H}(\mathrm{x},\mathrm{p}) &:= \langle \mathrm{p}, \sigma_0(\mathrm{x})\rangle + \frac{1}{2}\sum_{i=1}^{m} \langle \mathrm{p}, \sigma_i(\mathrm{x})\rangle^2 \\ &= \langle \mathrm{p}, \sigma_0(\mathrm{x})\rangle + \frac{1}{2}\left\langle \mathrm{p}, \left(\sigma\sigma^T\right)(\mathrm{x})\,\mathrm{p}\right\rangle.\end{aligned}$$

  Remark the driving Brownian motions $W^1, \ldots, W^m$ were assumed to be independent. Many stochastic models, notably in finance, are written in terms of correlated Brownian motions, i.e. with a non-trivial correlation matrix $\Omega = \left(\omega^{i,j} : 1 \le i, j \le m\right)$, where $d\left\langle W^i, W^j\right\rangle_t = \omega^{i,j} dt$. The Hamiltonian then becomes

$$\mathcal{H}(\mathrm{x},\mathrm{p}) = \langle \mathrm{p}, \sigma_0(\mathrm{x})\rangle + \frac{1}{2}\left\langle \mathrm{p}, \left(\sigma\Omega\sigma^T\right)(\mathrm{x})\,\mathrm{p}\right\rangle. \tag{12}$$

- **The Hamiltonian ODEs.** The following system of ordinary differential equations,

$$\begin{pmatrix} \dot{\mathrm{x}} \\ \dot{\mathrm{p}} \end{pmatrix} = \begin{pmatrix} \partial_{\mathrm{p}}\mathcal{H}(\mathrm{x}(t),\mathrm{p}(t)) \\ -\partial_{\mathrm{x}}\mathcal{H}(\mathrm{x}(t),\mathrm{p}(t)) \end{pmatrix}, \tag{13}$$

  gives rise to a solution flow, denoted by $\mathrm{H}_{t\leftarrow 0}$, so that

$$\mathrm{H}_{t\leftarrow 0}(\mathrm{x}_0, \mathrm{p}_0)$$

  is the unique solution to the above ODE with initial data $(\mathrm{x}_0, \mathrm{p}_0)$. Our standing (regularity) assumption are more than enough to guarantee uniqueness and local ODE existence. As in [8, p.37], the vector field $\left(\partial_{\mathrm{p}}\mathcal{H}, -\partial_{\mathrm{x}}\mathcal{H}\right)$ is complete, i.e.one has global existence. It can be useful to start the flow backwards with time-T terminal data, say $(\mathrm{x}_T, \mathrm{p}_T)$; we then write

$$\mathrm{H}_{t\leftarrow T}(\mathrm{x}_T, \mathrm{p}_T)$$

  for the unique solution to (13) with given time-T terminal data. Of course,

$$\mathrm{H}_{t\leftarrow T}\left(\mathrm{H}_{T\leftarrow 0}(\mathrm{x}_0, \mathrm{p}_0)\right) = \mathrm{H}_{t\leftarrow 0}(\mathrm{x}_0, \mathrm{p}_0).$$

- **Solving the Hamiltonian ODEs as boundary value problem.** Given the target manifold $N_{\mathrm{a}} = (\mathrm{a}, \cdot)$, the analysis in [10] requires solving the Hamiltonian ODEs (13) with mixed initial -, terminal - and transversality conditions,

$$\begin{aligned}&\mathrm{x}(0) = \mathrm{x}_0 \in \mathbb{R}^d, \\ &\mathrm{x}(T) = (\mathrm{y}, \cdot) \in \mathbb{R}^l \oplus \mathbb{R}^{d-l}, \\ &\mathrm{p}(T) = (\cdot, 0) \in \mathbb{R}^l \oplus \mathbb{R}^{d-l}.\end{aligned} \tag{14}$$

  Note that this is a $2d$-dimensional system of ordinary differential equations, subject to $d + l + (d - l) = 2d$ conditions. In general, boundary problems for such ODEs may have more than one, exactly one or no solution. In the present setting, there will always be one or more than one solution. After all, we know [10] that there exists at least one minimizing control h_0 and can be reconstructed via the solution of the Hamiltonian ODEs, as explained in the following step.

- **Finding the minimizing controls.** The Hamiltonian ODEs, as boundary value problem, are effectively first order conditions (for minimality) and thus yield *candidates* for the minimizing control $\mathrm{h}_0 = \mathrm{h}_0(\cdot)$, given by

$$\dot{\mathrm{h}}_0 = \begin{pmatrix} \langle \sigma_1(\mathrm{x}(\cdot)), \mathrm{p}(\cdot) \rangle \\ \dots \\ \langle \sigma_m(\mathrm{x}(\cdot)), \mathrm{p}(\cdot) \rangle \end{pmatrix}. \tag{15}$$

  Each such candidate is indeed admissible in the sense $\mathrm{h}_0 \in \mathcal{K}_\mathrm{a}$ but may fail to be a minimizer. We thus compute the energy $\|\mathrm{h}_0\|_H^2 = \mathcal{H}(x_0, p_0)$ for each candidate and identify those ("$\mathrm{h}_0 \in \mathcal{K}_\mathrm{a}^{\min}$") with minimal energy. The procedure via Hamiltonian flows also yields a unique $\mathrm{p}_0 = \mathrm{p}_0(\mathrm{h}_0)$. If $\sigma_0 = 0$ – as in our case – the energy is equal to $\mathcal{H}(x_0, p_0)$, otherwise the formula is slightly more complicated.

- **Checking non-focality.** By definition [10], x_0 is **non-focal** for $N = (\mathrm{y}, \cdot)$ along $\mathrm{h}_0 \in \mathcal{K}_\mathrm{a}^{\min}$ in the sense that, with $(\mathrm{x}_T, \mathrm{p}_T) := \mathrm{H}_{T \leftarrow 0}(\mathrm{x}_0, \mathrm{p}_0(\mathrm{h}_0)) \in \mathcal{T}^*\mathbb{R}^d$,

$$\partial_{(\mathfrak{z},\mathfrak{q})}|_{(\mathfrak{z},\mathfrak{q})=(0,0)} \pi \mathrm{H}_{0 \leftarrow T} \left(\mathrm{x}_T + \begin{pmatrix} 0 \\ \mathfrak{z} \end{pmatrix}, \mathrm{p}_T + (\mathfrak{q}, 0) \right)$$

  is non-degenerate (as $d \times d$ matrix; here we think of $(\mathfrak{z}, \mathfrak{q}) \in \mathbb{R}^{d-l} \times \mathbb{R}^l \cong \mathbb{R}^d$ and recall that π denotes the projection from $\mathcal{T}^*\mathbb{R}^d$ onto $\mathbb{R}^d$; in coordinates $\pi(\mathrm{x}, \mathrm{p}) = \mathrm{x}$). Note that in the point-point setting, $\mathrm{x}_T = \mathrm{y}$ is fixed and only perturbations of the arrival "velocity" p_T - without restrictions, i.e. without transversality condition - are considered. Non-degeneracy of the resulting map should then be called **non-conjugacy** (between two points; here: x_T and x_0). In the absence of the drift vector field σ_0, this is consistent with the usual meaning of non-conjugacy; after identifying tangent- and cotangent-space $\partial_\mathfrak{q}|_{\mathfrak{q}=0} \pi \mathrm{H}_{0 \leftarrow T}$ is precisely the differential of the exponential map.

- **The explicit marginal density expansion.** We then have

$$f^\varepsilon(\mathrm{y}, T) = e^{-c_1/\varepsilon^2} e^{c_2/\varepsilon} \varepsilon^{-l} (c_0 + O(\varepsilon)) \text{ as } \varepsilon \downarrow 0.$$

  with $c_1 = \Lambda(\mathrm{y})$. The second-order exponential constant c_2 then requires the solution of a finitely many ($\#\mathcal{K}_\mathrm{a}^{\min} < \infty$) auxiliary ODEs, cf. theorem 1.

4 Analysis of the Black–Scholes basket

For a general multi-dimensional Black-Scholes model, we have a Hamiltonian $\mathcal{H}(x, p) = \frac{1}{2} \left\langle p, (\sigma(x) \Omega \sigma(x)^T) p \right\rangle$, with $\sigma(x) = (\sigma^1 x^1, \dots, \sigma^m x^m)$. While the corresponding Hamiltonian ODEs can be solved in closed form, the boundary conditions lead to systems of non-linear equations, which we cannot solve explicitly any more. While numerical solutions are, of course, possible, we restrict ourselves to the extremely simple setting of Section 2, in order to keep maximal tractability.

Consequently, we have the Hamiltonian $\mathcal{H}(x, p) = \frac{1}{2} \left((\sigma x^1 p^1)^2 + (\sigma x^2 p^2)^2 \right)$. The solutions of the Hamiltonian ODEs started at (x_0, p_0) satisfy

$$H_{t \leftarrow 0}(x_0, p_0) = \begin{pmatrix} x_0^1 e^{\sigma^2 x_0^1 p_0^1 t} \\ x_0^2 e^{\sigma^2 x_0^2 p_0^2 t} \\ p_0^1 e^{-\sigma^2 x_0^1 p_0^1 t} \\ p_0^2 e^{-\sigma^2 x_0^2 p_0^2 t} \end{pmatrix}, \tag{16}$$

which can be easily seen from the observation that $\mathcal{H}$ is constant along solutions of the Hamiltonian ODEs together with symmetry between (x^1, p^1) and (x^2, p^2). This immediately implies that the inverse flow is given by

$$H_{0\leftarrow t}(x_t, p_t) = \begin{pmatrix} x_t^1 e^{-\sigma^2 x_t^1 p_t^1 t} \\ x_t^2 e^{-\sigma^2 x_t^2 p_t^2 t} \\ p_t^1 e^{\sigma^2 x_t^1 p_t^1 t} \\ p_t^2 e^{\sigma^2 x_t^2 p_t^2 t} \end{pmatrix}. \tag{17}$$

Now we introduce the boundary conditions. Note that, contrary to Theorem 1, we now project to the linear subspace $\{x : x^1 + x^2 = K\}$. Thus, the terminal condition on x translates into $x_T^1 + x_T^2 = K$ – we need to end at the target manifold –, whereas the transversality condition translates to p_T being orthogonal to the target manifold. Evaluating these conditions at $T = 1$, we get

$$\begin{aligned} x_0^1 &= S_0^1 = 1, \\ x_0^2 &= S_0^2 = 1, \\ x_1^1 + x_1^2 &= K, \\ p_1^1 - p_1^2 &= 0. \end{aligned}$$

By symmetry, it is clear that the optimal configuration must satisfy $x_1^* = (K/2, K/2)$. Inserting this value into the first two components of (16), we obtain the equation

$$\frac{K}{2} = e^{\sigma^2 p_0^i} \iff p_0^i = \log\left(\frac{K}{2}\right)/\sigma^2, \quad i = 1, 2.$$

This implies that $p_1^* = \left(\frac{2}{\sigma^2 K}\log(K/2), \frac{2}{\sigma^2 K}\log(K/2)\right)$. Moreover, we see that the minimizing control satisfies

$$\dot{h}_0(t) = \begin{pmatrix} \sigma x^1(t) p^1(t) \\ \sigma x^2(t) p^2(t) \end{pmatrix} = \begin{pmatrix} \sigma p_0^1 \\ \sigma p_0^2 \end{pmatrix} = \begin{pmatrix} \frac{\log(K/2)}{\sigma} \\ \frac{\log(K/2)}{\sigma} \end{pmatrix}, \tag{18}$$

see (15), implying that the minimal energy is given by

$$\Lambda(K) = \frac{1}{2}\|h_0\|_H^2 = \frac{\log(K/2)^2}{\sigma^2} = \mathcal{H}(x_0, p_0). \tag{19}$$

Regarding focality, we have to check that the matrix:

$$M(x_1, p_1) := \begin{pmatrix} \frac{\partial}{\partial\epsilon}\big|_{\epsilon=0} H_{0\leftarrow 1}^1(x_1 + \epsilon(1,-1), p_1) & \frac{\partial}{\partial\eta}\big|_{\eta=0} H_{0\leftarrow 1}^1(x_1, p_1 + \eta(1,1)) \\ \frac{\partial}{\partial\epsilon}\big|_{\epsilon=0} H_{0\leftarrow 1}^2(x_1 + \epsilon(1,-1), p_1) & \frac{\partial}{\partial\eta}\big|_{\eta=0} H_{0\leftarrow 1}^2(x_1, p_1 + \eta(1,1)) \end{pmatrix} \tag{20}$$

is non-degenerate when evaluated at the optimal configuration (x_1^*, p_1^*). A simple calculation shows that

$$M(x_1, p_1) = \begin{pmatrix} e^{-\sigma^2 x_1^1 p_1^1} - x_1^1 p_1^1 \sigma^2 e^{-\sigma^2 x_1^1 p_1^1} & -\sigma^2 (x_1^1)^2 e^{-\sigma^2 x_1^1 p_1^1} \\ -e^{-\sigma^2 x_1^2 p_1^2} + x_1^2 p_1^2 \sigma^2 e^{-\sigma^2 x_1^2 p_1^2} & -\sigma^2 (x_1^2)^2 e^{-\sigma^2 x_1^2 p_1^2} \end{pmatrix},$$

implying that

$$M(x_1^*, p_1^*) = \begin{pmatrix} \frac{2}{K}(1 - \log(K/2)) & -\frac{\sigma^2 K}{2} \\ \frac{2}{K}(-1 + \log(K/2)) & -\frac{\sigma^2 K}{2} \end{pmatrix},$$

and we can conclude that

$$\det M(x_1^*, p_1^*) = 2\sigma^2 \left(\log(K/2) - 1\right),$$

which is zero if and only if $K = 2e$. We summarize the results of this calculation as follows:

- In the generic case $K \neq 2e$, the non-focality condition of Theorem 1 holds true, and we obtain (from Corollary 3) the following (short time) density expansion of $B_T = \exp(\sigma W_T^1) + \exp(\sigma W_T^2)$, expansion
$$K \mapsto \exp\left(-\frac{\Lambda(K)}{T}\right) \frac{1}{\sqrt{T}} \left(1 + O(T)\right)$$
When specialized to unit volatility, we precisely find (1a).
- For $K = 2e$, the initial stock price is focal for the minimizing configuration, so the non-focality condition of Theorem 1 fails. And indeed, we *want* it to fail for the actual expansion in this case, namely (1b), is not at all of the generic form predicted by our theorem.

Remark 4. It is immediate to use this analysis to deal also with the case of non-unit (but identical) spots $S_0^1 = S_0^2$ by scaling the Black-Scholes dynamics accordingly, i.e., by replacing K with K/S_0^1. Hence, in this case focality happens when $\log\left(\frac{K}{2S_0^1}\right) = 1$, i.e., when $K = 2S_0^1 e$.

5 Extensions: correlation, local and stochastic vol

5.1 Analysis of the Black–Scholes basket, small noise

In section 4 we analyzed the density of a simple Black–Scholes basket with dynamics

$$dB_t = S_t^1 \sigma dW_t^1 + S_t^2 \sigma dW_t^2.$$

As explained in Section 3 the analysis is really based on a small noise (small vol) expansion of

$$dB_t^\epsilon = S_t^{1,\epsilon} \sigma \epsilon dW_t^1 + S_t^{2,\epsilon} \sigma \epsilon dW_t^2,$$

run til time $T = 1$. Consider now a situation with small rates, also of order ϵ. In other words,

$$dS_t^{i,\epsilon} = r S_t^{i,\epsilon} \epsilon dt + S_t^{i,\epsilon} \sigma \epsilon dW^i,$$

and then $B_t^\epsilon = S_t^{1,\epsilon} + S_t^{2,\epsilon}$ as before. We still assume $S_0^i = 1$. A look at Theorem 1 (now we cannot use Corollary 3) reveals that the entire leading order computation remains unchanged (at least at unit time and with trivial changes otherwise). The resulting (now: small noise) density expansion of of $B_T^\epsilon|_{T=1}$ is more involved and takes the form

$$K \mapsto \exp\left(-\frac{\Lambda(K)}{\epsilon^2}\right) \exp\left(\frac{2r\log(K/2)}{\sigma^2 \log(2)\epsilon}\right) \frac{1}{\epsilon} \left(1 + O(\epsilon)\right). \tag{21}$$

Here $\Lambda(K)$ is given in closed form, cf. 19, so that $\Lambda'(K) = \frac{2\log(K/2)}{\sigma^2 K}$ is also explicitly known. Furthermore, h_0 is (still) given by (18), so that

$$\phi_t^{h_0} = \begin{pmatrix} (K/2)^t \\ (K/2)^t \end{pmatrix}.$$

Thus, the ODE for $\hat{X}$ (see Theorem 1) is given by

$$\frac{d\hat{X}_t}{dt} = \log(K/2)\hat{X}_t + r\begin{pmatrix}(K/2)^t\\(K/2)^t\end{pmatrix}, \quad \hat{X}_0 = \hat{x}_0 = 0,$$

which has the solution

$$\hat{X}^i_t = r\left(1 - \left(\frac{1}{2}\right)^t\right)\frac{K^t}{\log 2},$$

implying that $\hat{Y}_1 = \hat{X}^1_1 + \hat{X}^2_1 = rK/\log(2)$. Thus, the second exponential term has the form given above.

5.2 Basket analysis under local, stochastic vol etc.

One can immediately write down the Hamiltonian associated to, say two, or $d > 2$ assets, each of which is governed by local vol dynamics or stochastic vol, based on additional factors. In general, however, one will be stuck with the analysis of the resulting boundary value problem for the Hamiltonian ODEs; numerical (e.g. shooting) methods will have to be used. In some models, including the Stein–Stein model, we believe (due to the analysis carried out in [11]) that, in special cases, closed form answers are possible but we will not pursue this here. Instead, we continue with a few more computation in the Black–Scholes case for d assets.

5.3 Multi-variate Black-Scholes models

In the multi-variate case $d > 2$ of a general, d-dimensional Black Scholes model with correlation matrix (ρ_{ij}), the Hamiltonian has the form

$$\mathcal{H}(x,p) = \frac{1}{2}\sum_{i,j=1}^{d}\rho_{ij}\sigma^i p^i x^i \sigma^j x^j p^j.$$

Thus, the Hamiltonian ODEs have the form

$$\dot{x}^l = \sigma^l x^l \sum_{i=1}^{d}\rho_{li}\sigma^i p^i x^i, \quad i = 1,\dots,d$$
$$\dot{p}^l = -\sigma^l p^l \sum_{i=1}^{d}\rho_{li}\sigma^i p^i x^i, \quad i = 1,\dots,d.$$

Consequently, it is again easy to see that $\frac{\partial}{\partial t}x^l(t)p^l(t) = 0$, implying that $x^l(t)p^l(t) = x^l_0 p^l_0$. The Hamiltonian flow has the form

$$H_{t\leftarrow 0}(x_0,p_0) = \begin{pmatrix}\left(x^l_0\exp\left[\sigma^l\left(\sum_{i=1}^d\rho_{li}\sigma^i p^i_0 x^i_0\right)t\right]\right)_{l=1}^d\\ \left(p^l_0\exp\left[-\sigma^l\left(\sum_{i=1}^d\rho_{li}\sigma^i p^i_0 x^i_0\right)t\right]\right)_{l=1}^d\end{pmatrix}. \tag{22}$$

Using again that $p^l(t)x^l(t) = p^l(0)x^l(0)$ for any l, we obtain the inverse Hamiltonian flow

$$H_{0\leftarrow t}(x_t,p_t) = \begin{pmatrix}\left(x^l_t\exp\left[-\sigma^l\left(\sum_{i=1}^d\rho_{li}\sigma^i p^i_t x^i_t\right)t\right]\right)_{l=1}^d\\ \left(p^l_t\exp\left[\sigma^l\left(\sum_{i=1}^d\rho_{li}\sigma^i p^i_t x^i_t\right)t\right]\right)_{l=1}^d\end{pmatrix}. \tag{23}$$

The boundary conditions – at $T = 1$ – are now given by

$$x_0 = S_0 \tag{24a}$$

$$\sum_{l=1}^{d} x^l(1) = K \tag{24b}$$

$$p^1(1) = p^2(1) = \cdots = p^d(1). \tag{24c}$$

Indeed, the transversality condition (24c) says that the final momentum $p(1)$ is orthogonal to the surface $\left\{ \sum_{l=1}^{d} y^l = K \right\}$, whose tangent space is spanned by the collection of vectors $\mathbf{e}_1 - \mathbf{e}_l$, $l = 2, \ldots, d$, with $\mathbf{e}_1, \ldots, \mathbf{e}_d$ the standard basis of $\mathbb{R}^d$. The equations (24) are certainly not difficult to solve numerically, but an explicit solution is not available, neither in the general case nor in the case of d uncorrelated assets.

Remark 5. The main point of this calculation is that while explicit solutions are no longer possible in a general Black-Scholes model, the phenomenon (1) potentially appears in all Black-Scholes models. Moreover, we stress that the non-focality conditions are easily checked numerically.

Remark 6. Note that the discretely monitored Asian option can be considered as a special case of a basket option on correlated assets. Indeed, let us consider an option on

$$\frac{1}{N} \sum_{i=1}^{N} S_{t_i}, \text{ with (for simplicity) } t_i = i\Delta t, \quad i = 1, \ldots, N.$$

For each individual $i \in \{1, \ldots, N\}$ we have, for fixed $\Delta t > 0$, the equality in law

$$S_{t_i} = S_0 e^{\sigma B_{i\Delta t} - \frac{1}{2}\sigma^2 i\Delta t} = S_0 e^{\sigma^i W^i_{\Delta t} - \frac{1}{2}(\sigma^i)^2 \Delta t}$$

for $\sigma^i := \sqrt{i}\sigma$ and $W^i_{\Delta t} := B_{i\Delta t}/\sqrt{i}$. In law, the vector $\left(W^1_{\Delta t}, \ldots, W^N_{\Delta t}\right)$ corresponds to the marginal distribution of an N-dimensional Brownian motion at time Δt with correlation $\rho_{ij} = \frac{\min(i,j)}{\sqrt{ij}}$, $1 \le i, j \le N$. Thus, the Asian option corresponds to an option on the basket with $S^i_0 \equiv S_0$, σ^i as above and a correlation matrix ρ_{ij} with maturity Δt. Moreover, the asymptotic expansion of the price of the Asian option as $\Delta t \to 0$ corresponds to the short-time asymptotics of the basket.

Remark 7. A small-noise asymptotic expansion of the continuous Asian option on $\int_0^T S_t dt$ is also possible by the techniques of Section 3 (with ellipticity conditions replaced by weak Hörmander conditions). Essentially, this is equivalent to letting $N \to \infty$ in Remark 6 – but more direct.

As in the two-dimensional case, the boundary conditions can be solved explicitly in the fully symmetric case, when $\sigma^l \equiv \sigma$ and, say, $S^l_0 \equiv 1$. Then the optimal configuration satisfies

$$x^*_0 = (1, \ldots, 1)^T, \quad x^*_1 = (K/d, \ldots, K/d)^T$$

$$p^*_0 = \left(\frac{\log(K/d)}{\sigma^2}, \ldots, \frac{\log(K/d)}{\sigma^2} \right)^T, \quad p^*_1 = \left(\frac{d}{\sigma^2 K} \log(K/d), \ldots, \frac{d}{\sigma^2 K} \log(K/d) \right)^T.$$

Introducing

$$\mathfrak{q} = \epsilon_1 \begin{pmatrix} 1 \\ 1 \\ \vdots \\ 1 \end{pmatrix}, \quad \mathfrak{z} = \begin{pmatrix} \epsilon_2 + \cdots + \epsilon_d \\ -\epsilon_2 \\ \vdots \\ -\epsilon_d \end{pmatrix},$$

we obtain (for the case of d uncorrelated assets)

$$\begin{aligned} M(x_1, p_1) &:= \partial_{(\mathfrak{z},\mathfrak{q})}\big|_{(\mathfrak{z},\mathfrak{q})=0} \pi H_{0\leftarrow 1}(x_1 + \mathfrak{z}, p_1 + \mathfrak{q}) \\ &= \begin{pmatrix} a_1 & \mathbf{b} \\ \mathbf{a} & G \end{pmatrix}, \end{aligned}$$

where $\mathbf{a} = (a_2, \ldots, a_d)^T \in \mathbb{R}^{(d-1)\times 1}$, $\mathbf{b} = b(1, \ldots, 1) \in \mathbb{R}^{1\times(d-1)}$, $G = \operatorname{diag}(g_2, \ldots, g_d) \in \mathbb{R}^{(d-1)\times(d-1)}$ with

$$\begin{aligned} a_l &= -(\sigma^l)^2 (x_1^l)^2 e^{-(\sigma^l)^2 p_1^l x_1^l}, \quad l = 1, \ldots d, \\ b &= \left[1 - (\sigma^1)^2 x_1^1 p_1^1\right] e^{-(\sigma^1)^2 p_1^1 x_1^1}, \\ g_l &= -\left[1 - (\sigma^l)^2 x_1^l p_1^l\right] e^{-(\sigma^l)^2 p_1^l x_1^l}, \quad l = 2, \ldots d. \end{aligned}$$

In the symmetric case, we can evaluate M at the optimal configuration and obtain

$$M(x_1^*, p_1^*) = \begin{pmatrix} -\sigma^2 \frac{K}{d} & [1 - \log(K/d)] \frac{d}{K} & \cdots & [1 - \log(K/d)] \frac{d}{K} \\ -\sigma^2 \frac{K}{d} & -[1 - \log(K/d)] \frac{d}{K} & \cdots & 0 \\ \vdots & \vdots & \ddots & \vdots \\ -\sigma^2 \frac{K}{d} & 0 & \cdots & -[1 - \log(K/d)] \frac{d}{K} \end{pmatrix},$$

whose determinant can be seen to be

$$\det M(x_1^*, p_1^*) = (-1)^d \sigma^2 K \left[(1 - \log(K/d)) \frac{d}{K}\right]^{d-1}.$$

Thus, the non-focality condition fails if and only if $K = de$. Moreover, we obtain the energy

$$\Lambda(K) = \mathcal{H}(x_0^*, p_0^*) = \frac{d}{2} \frac{\log(K/d)^2}{\sigma^2}.$$

A A geometric approach to focality

Consider the Black Scholes model

$$dS_t^i = \sigma^i S_t^i dW_t^i, \quad \left\langle dW^i, dW^j \right\rangle_t = \rho_{i,j} dt.$$

We change parameters $\mathbf{S} \to \mathbf{y} \to \mathbf{x}$, by

$$y^i := \frac{\log\left(\frac{S^i}{S_0^i}\right)}{\sigma^i}, \quad x^i = L_{ip} y^p, \quad i = 1, \ldots, d,$$

where $\boldsymbol{\rho}$ denotes the correlation matrix of $\mathbf{W}$ and $\rho = LL^T$ its Cholesky factorization. Obviously, $S^i = S_0^i e^{\sigma_i y^i}$. and in terms of the $\mathbf{x}$-coordinates we have

$$\begin{aligned} x^i = x^i(\mathbf{F}) &= L_{ip} \log\left(S^p / S_0^p\right) / \sigma^p, \\ S^i = S^i(\mathbf{x}) &= S_0^i e^{\sigma_i L^{ip} x^p}. \end{aligned}$$

The advantage of using the chart $\mathbf{x}$ is that the corresponding Riemannian metric tensor is the usual Euclidean metric tensor. Thus, we simply have

$$d(\mathbf{S}_0, \mathbf{S}) = |\mathbf{x}_0 - \mathbf{x}|$$

and the geodesics are straight lines as seen from the $\mathbf{x}$-chart. Note furthermore that $\mathbf{S} = \mathbf{S}_0$ is transformed to $\mathbf{x} = \mathbf{0}$.

The payoff function of the option is given by $\left(\sum w_i S_T^i - K\right)^+$. We normalize $w_i \equiv 1$ and $T \equiv 1$. The strike surface $F = \left\{\mathbf{S} \in \mathbb{R}_+^d \,\middle|\, \sum_{i=1}^d S^i = K\right\}$, which is (a sub-set of) a hyperplane in $\mathbf{S}$ coordinates is, however, transformed to a much more complicated submanifold in $\mathbf{x}$ coordinates. Re-phrasing the equation $\sum_i S^i = K$ in $\mathbf{y}$-coordinates and solving for y^d gives

$$y^d = \log\left[\left(K - \sum_{i=1}^{d-1} S_0^i e^{\sigma^i \sum_{p=1}^d L^{ip} x^p}\right) / S_0^d\right] / \sigma^d,$$

with $(L^{ij}) = (L_{ij})^{-1}$, which implies – using that L and L^{-1} are lower-triangular matrices –

$$L^{dd} x^d = \log\left[\left(K - \sum_{i=1}^{d-1} S_0^i e^{\sigma^i \sum_{p=1}^i L^{ip} x^p}\right) / S_0^d\right] / \sigma^d - \sum_{k=1}^{d-1} L^{dk} x^k.$$

For sake of clarity, let us introduce the notation $\mathbf{q} = (q^1, \ldots, q^{d-1}) := (x^1, \ldots, x^{d-1})$. A parametrization of the strike surface F is then given by the map $\varphi : U \subset \mathbb{R}^{d-1} \to \mathbb{R}^d$ with

$$U := \left\{\mathbf{q} \in \mathbb{R}^{d-1} \,\middle|\, \sum_{i=1}^{d-1} S_0^i e^{\sigma^i \sum_{p=1}^i L^{ip} q^p} < K\right\},$$

and

$$\varphi(\mathbf{q}) := \left(\mathbf{q},\ \frac{1}{L^{dd}} \left\{\log\left[\left(K - \sum_{i=1}^{d-1} S_0^i e^{\sigma^i \sum_{p=1}^i L^{ip} q^p}\right) / S_0^d\right] / \sigma^d - \sum_{k=1}^{d-1} L^{dk} q^k\right\}\right).$$

Note that by the change of coordinates, we are implicitly assuming that $S^i > 0$ for all i. Moreover, the standard basis $\mathbf{e}_1(\mathbf{p}), \ldots, \mathbf{e}_{d-1}(\mathbf{p})$ of the tangent space $T_{\mathbf{p}}F$ to F at $\mathbf{p} = \varphi(\mathbf{q})$ is given by the columns of the Jacobi matrix of φ evaluated at $\mathbf{q}$, more precisely we have

$$\mathbf{e}_i(\mathbf{p}) = \left((\delta_i^j)_{j=1}^{d-1},\ -\frac{1}{L^{dd}}\left[\frac{1}{\sigma^d} \frac{\sum_{j=i}^{d-1} \sigma^j L^{ji} S_0^j e^{\sigma^j \sum_{r=1}^j L^{jr} q^r}}{K - \sum_{j=1}^{d-1} S_0^j e^{\sigma^j \sum_{r=1}^j L^{jr} q^r}} + L^{di}\right]\right)$$

for $i = 1, \ldots, d-1$ and $\mathbf{p} = \varphi(\mathbf{q})$. Consequently, the normal vector field N to S at $\mathbf{p} = \varphi(\mathbf{q})$ is given by

$$N(\mathbf{p}) = \alpha(\mathbf{p}) \left(\left(\frac{1}{L^{dd}}\left[\frac{1}{\sigma^d} \frac{\sum_{j=i}^{d-1} \sigma^j L^{ji} S_0^j e^{\sigma^j \sum_{r=1}^j L^{jr} q^r}}{K - \sum_{j=1}^{d-1} S_0^j e^{\sigma^j \sum_{r=1}^j L^{jr} q^r}} + L^{di}\right]\right)_{i=1}^{d-1}, 1\right) = N \circ \varphi(\mathbf{q}),$$

where α is a normalization factor guaranteeing that $|N(\mathbf{p})| = 1$, i.e.,

$$\alpha(\mathbf{p}) = \left(1 + \sum_{i=1}^{d-1} \frac{1}{(L^{dd})^2}\left[\frac{1}{\sigma^d} \frac{\sum_{j=i}^{d-1} \sigma^j L^{ji} S_0^j e^{\sigma^j \sum_{r=1}^j L^{jr} q^r}}{K - \sum_{j=1}^{d-1} S_0^j e^{\sigma^j \sum_{r=1}^j L^{jr} q^r}} + L^{di}\right]^2\right)^{-1/2}.$$

The *Weingarten map* or *shape operator* $L_{\mathbf{p}} : T_{\mathbf{p}}F \to T_{\mathbf{p}}F$ is defined by

$$L_{\mathbf{p}}\left(d\varphi_{\varphi^{-1}(\mathbf{p})}(\mathbf{v})\right) = -d(N \circ \varphi)(\varphi^{-1}(\mathbf{p})) \cdot \mathbf{v},$$

$\mathbf{v} \in \mathbb{R}^{d-1} = T_{\varphi^{-1}(\mathbf{p})}U$, see [13]. In other words, for $\varphi(\mathbf{q}) = \mathbf{p}$, we interpret N as a map in $\mathbf{q}$ and $-L_{\mathbf{p}}$ is than the directional derivative of that map. We study the Weingarten map since it gives us the curvature of the surface F. Indeed, the eigenvalues $k_1(\mathbf{p}), \ldots, k_{d-1}(\mathbf{p})$ of the linear map $L_{\mathbf{p}} : T_{\mathbf{p}}F \to T_{\mathbf{p}}F$ are called *principal curvatures* of F. Then the *focal points* of F at $\mathbf{p}$ are given by

$$\{\mathbf{p} + \frac{1}{k_i(\mathbf{p})}N(\mathbf{p}) | 1 \leq i \leq d-1 \text{ such that } k_i(\mathbf{p}) \neq 0\}.$$

In order to compute the eigenvalues of the shape operator, we need to compute the representation of $L_{\mathbf{p}}$ in the standard basis $(\mathbf{e}_1(\mathbf{p}), \ldots, \mathbf{e}_{d-1}(\mathbf{p}))$. Let us denote this matrix by $\overline{L}(\mathbf{p})$, then we obviously have

$$\overline{L}(\varphi(\mathbf{q}))_{ij} = -\langle \frac{\partial}{\partial q^j}(N \circ \varphi)(\mathbf{q}), \mathbf{e}_i(\varphi(\mathbf{q}))\rangle, \quad i, j = 1, \ldots, d-1.$$

The principal curvatures $k_1(\mathbf{p}), \ldots, k_{d-1}(\mathbf{p})$ are, thus, the eigenvalues of the $(d-1)$-dimensional matrix $\overline{L}(\mathbf{p})$.

Since the calculations become too complicated in the general case, we now again concentrate on the case of *two uncorrelated* assets, i.e., $d = 2$ and $\boldsymbol{\rho} = L = I_2$. In this case, we have

$$\mathbf{e}_1(\mathbf{p}) = \left(1, -\frac{\sigma^1}{\sigma^2}\frac{S_0^1 e^{\sigma^1 q^1}}{K - S_0^1 e^{\sigma^1 q^1}}\right),$$

$$N(\varphi(\mathbf{q})) = \frac{1}{\sqrt{(\sigma^1)^2(S_0^1)^2 e^{2\sigma^1 q^1} + (\sigma^2)^2\left(K - S_0^1 e^{\sigma^1 q^1}\right)^2}}\left(\sigma^1 S_0^1 e^{\sigma^1 q^1}, \sigma^2\left(K - S_0^1 e^{\sigma^1 q^1}\right)\right).$$

Thus, the Weingarten map is given by

$$L_{\mathbf{p}}(v\mathbf{e}_1(\mathbf{p})) = v\kappa(\mathbf{p})\mathbf{e}_1(\mathbf{p}),$$

where for $\mathbf{q} = (q^1) \in \mathbb{R}$

$$\kappa(\varphi(\mathbf{q})) = k_1(\varphi(\mathbf{q})) = \frac{K(\sigma^1)^2(\sigma^2)^2 S_0^1 e^{\sigma^1 q^1}\left(S_0^1 e^{\sigma^1 q^1} - K\right)}{\left[(\sigma^1)^2(S_0^1)^2 e^{2\sigma^1 q^1} + (\sigma^2)^2\left(S_0^1 e^{\sigma^1 q^1} - K\right)^2\right]^{3/2}}$$

is the *curvature* of the curve F in $\mathbb{R}^2$. We see that $\kappa = 0$ if and only if $K = S_0^1 e^{\sigma^1 q^1}$, i.e., at the boundary of the surface F. Otherwise, κ is negative.

Here, both components of $N(\mathbf{p})$ are positive on F. Consequently, for any $\mathbf{p} = \varphi(\mathbf{q}) \in S$ there is precisely one focal point $\tilde{\mathfrak{f}} = \tilde{\mathfrak{f}}(\mathbf{p}) \in \mathbb{R}^2$, which is given by

$$\tilde{\mathfrak{f}}^1 = q^1 + \frac{S_0^1 e^{\sigma^1 q^1}\left[2(\sigma^2)^2 K - ((\sigma^1)^2 + (\sigma^2)^2)S_0^1 e^{\sigma^1 q^1}\right] - (\sigma^2)^2 K^2}{\sigma^1(\sigma^2)^2 K\left(K - S_0^1 e^{\sigma^1 q^1}\right)},$$

$$\tilde{\mathfrak{f}}^2 = \frac{1}{\sigma^2}\log\left(\frac{K - S_0^1 e^{\sigma^1 q^1}}{S_0^2}\right) + 2\frac{\sigma^2}{(\sigma^1)^2} - \frac{\sigma^2 K e^{-\sigma^1 q^1}}{(\sigma^1)^2 S_0^1} - \frac{((\sigma^1)^2 + (\sigma^2)^2)S_0^1 e^{\sigma^1 q^1}}{(\sigma^1)^2\sigma^2 K}.$$

Denoting $\mathbf{p} = (x^1, x^2)$ and re-introducing the short-cut notation $S^i = S_0^i e^{\sigma^i x^i}$, $i = 1, 2$, (noting that $S^1 + S^2 = K$) we can express $\mathfrak{f}$ as

$$\mathfrak{f}^1 = x^1 + \frac{S^1\left[2(\sigma^2)^2 K - ((\sigma^1)^2 + (\sigma^2)^2)S^1\right] - (\sigma^2)^2 K^2}{\sigma^1(\sigma^2)^2 K S^2},$$
$$\mathfrak{f}^2 = x^2 + \frac{S^1\left[2(\sigma^2)^2 K - ((\sigma^1)^2 + (\sigma^2)^2)S^1\right] - (\sigma^2)^2 K^2}{(\sigma^1)^2\sigma^2 K S^1}.$$

In the current setting, let $\mathbf{q}^*$ be the optimal configuration in $\mathbf{q}$-coordinates, i.e., the point on F with smallest Euclidean norm. Then the non-focality condition of Theorem 1 is satisfied, if 0 is not a focal point to $\varphi(\mathbf{q}^*)$, see the discussion in the proof of [10, Prop. 6].

Remark 8. As both components of the normal vector N are non-negative on F and the curvature κ is negative, $\mathbf{0}$ can only be a focal point if F has a non-empty intersection with the positive quadrant. Inserting into the parametrization of F, we see that this can only be the case if $K > S_0^1 + S_0^2$. In other words: if the option is in the money, then the non-focality condition is always satisfied (in the two-dimensional, uncorrelated case).

Let us again use the parameters of Section 2, i.e., $S_0^1 = S_0^2 = 1$, $\sigma^1 = \sigma^2 = \sigma$. Then we consider $\mathbf{S}^* = (K/2, K/2)$, which translates into $\mathbf{x}^* = \left(\frac{\log(K/2)}{\sigma}, \frac{\log(K/2)}{\sigma}\right)$. Inserting into the formulas for the focal points, we obtain

$$\mathfrak{f}^1(\mathbf{x}^*) = \mathfrak{f}^2(\mathbf{x}^*) = \frac{\log\left(\frac{K}{2}\right) - 1}{\sigma}.$$

So, 0 is focal to the optimal configuration, if and only if

$$K = 2e,$$

and we recover, once more, the results of Section 2 and Section 4 – recall that $\mathbf{S}_0$ corresponds to 0 in $\mathbf{x}$-coordinates.

In Figure 1 and 2 the focal points are visualized for two different configurations of two uncorrelated baskets. We plot the surface F as a submanifold of $\mathbb{R}^2$. We have seen above that for any $\mathbf{p} \in F$ there is precisely one focal point $\mathfrak{f}(\mathbf{p})$. Hence, we additionally plot the surface $\{\mathfrak{f}(\mathbf{p}) | \mathbf{p} \in F\}$ – more precisely, part of this surface. In Figure 1 we show the case constructed above where the non-focality condition is violated. In Figure 2 the option is ITM. As explained above, in the ITM case the manifold F does not intersect the positive quadrant, implying that the non-focality condition is satisfied.

References

[1] M. Avellaneda, D. Boyer-Olson, J.Busca, P. Friz: Application of large deviation methods to the pricing of index options in finance, *Comptes Rendus de l'Académie des Sciences - Series I - Mathematique* (2003).

[2] M. Avellaneda, D. Boyer-Olson, J.Busca, P. Friz: Reconstructing volatility, RISK (2004).

[3] C. Bayer and P. Laurence, Asymptotics beats Monte-Carlo: the case of correlated local vol baskets. Forthcoming in *Communications on Pure and Applied Mathematics*.

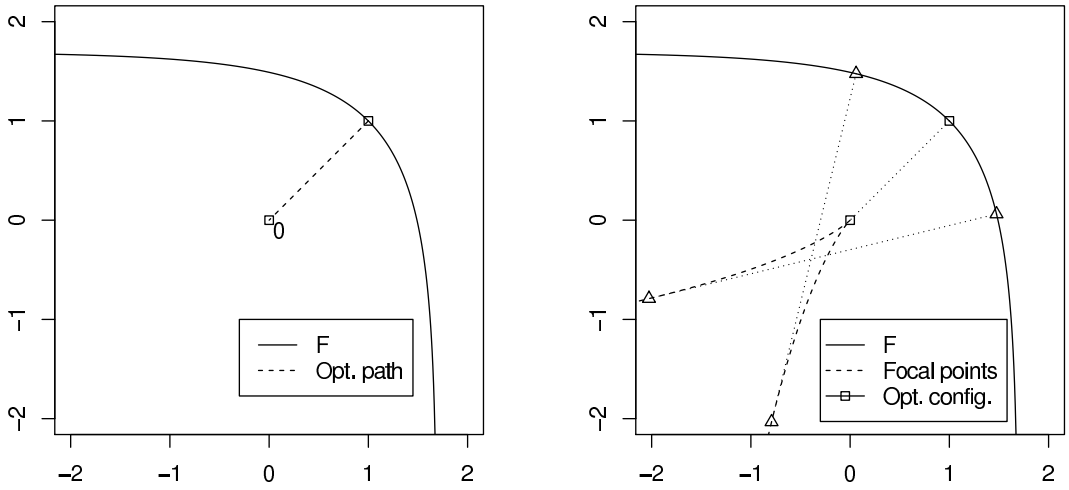

(a) Optimal configuration (b) Focal points

Figure 1: Optimal configuration and focal points for two independent assets with $\sigma^1 = \sigma^2 = 1$, $\mathbf{S}_0 = (1, 1)$, $K = 2e$.
(A) The dashed line depicts the optimal path between the spot price $\mathbf{S}_0$ (0 in the $\mathbf{q}$-chart) and the optimal configuration.
(B) Dotted lines connect some selected points on the manifold F with the corresponding focal points. Points marked with a triangle visualize the construction of the focal points. We see that 0 is, indeed, focal to the optimal configuration.

[4] Benaim, Friz: Regular Variation and Smile Asymptotics, Math. Finance Vol. 19 no 1. (2009), 1-12

[5] G. Ben Arous. Développement asymptotique du noyau de la chaleur hypoelliptique hors du cut-locus. *Annales Scientifiques de l'Ecole Normale Supérieure*, 4 (21): 307-331, 1988.

[6] G. Ben Arous. Methods de Laplace et de la phase stationnaire sur l'espace de Wiener. *Stochastics*, 25: 125-153, 1988.

[7] H. Berestycki, J. Busca, and I. Florent. Computing the implied volatility in stochastic volatility models. Communications on Pure and Applied Mathematics, 57(10):1352-1373, 2004.

[8] J.M. Bismut. Malliavin Calculus and Large Deviations. 1984

[9] S. de Marco, P.K. Friz. aradhan's formula for projected diffusion and local volatility. Preprint 2013.

[10] J.D. Deuschel, P.K. Friz, A. Jacquier, S. Violante. Marginal density expansions for diffusions and stochastic volatility, part I: Theoretical Foundations. Communications on Pure and Applied Mathematics, to appear.

[11] J.D. Deuschel, P.K. Friz, A. Jacquier, S. Violante. Marginal density expansions for diffusions and stochastic volatility, part II: Applications. Communications on Pure and Applied Mathematics, to appear.

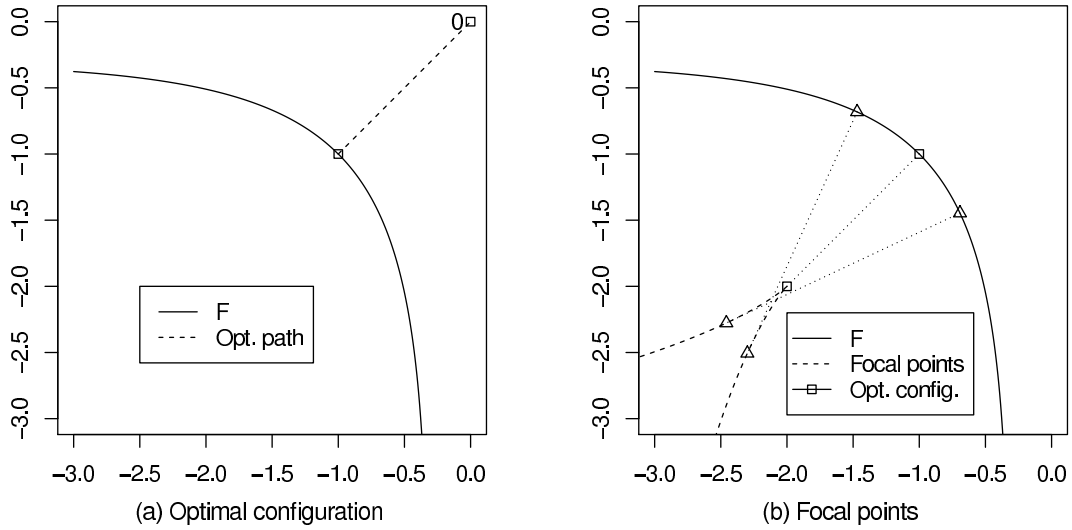

(a) Optimal configuration (b) Focal points

Figure 2: Optimal configuration and focal points for two independent assets with $\sigma^1 = \sigma^2 = 1$, $\mathbf{S}_0 = (1, 1)$, $K = 2/e$.
(A) The dashed line depicts the optimal path between the spot price $\mathbf{S}_0$ (0 in the $\mathbf{q}$-chart) and the optimal configuration.
(B) Dotted lines connect some selected points on the manifold F with the corresponding focal points. Points marked with a triangle visualize the construction of the focal points. This example illustrates the fact that the non-focality condition always holds when the basket option is in the money.

[12] J.D. Deuschel and D.W. Stroock. Large Deviations. Volume 342 of AMS/Chelsea Series. 2000

[13] M.P. do Carmo. Differential geometry of curves and surfaces. Prentice-Hall, 1976.

[14] D. Dufresne, The log-normal approximation in financial and other computations, Advances in Applied Probability 36, pgs 747-773, 2004.

[15] M. Freidlin and A.D. Wentzell. Random perturbations of dynamical systems. Grundlehren der Mathematischen Wissenschaften (Second edition ed.). New York: Springer-Verlag, 1998.

[16] P. Friz, S. Gerhold, A. Gulisashvili and S. Sturm. Refined implied volatility expansions in the Heston model. Quant. Finance, Volume 11, Issue 8, 1151-1164, 2011.

[17] K. Gao and R. Lee. Asymptotics of implied volatility to arbitrary order. Preprint available at http://ssrn.com/abstract=1768383, 2011.

[18] Gatheral, Jim; The Volatilty Surface. Wiley Finance, 2006.

[19] Gatheral, Jim; Further Developments in Volatility Derivatives Modeling. Presentation 2008. Available on www.math.nyu.edu/fellows_fin.../gatheral/FurtherVolDerivatives2008.pdf

[20] Gatheral, Jim; Hsu, Elton P.; Laurence, Peter; Ouyang, Cheng; Wang, Tai-Ho. Asymptotics of Implied Vol in Local Vol Models. *Math. Finance*, Volume 22, Issue 4, pages 591–620, October 2012.

[21] A. Gulisashvili. Analytically tractable stochastic stock price models, Springer finance, Springer London 2012.

[22] A. Gulisashvili and E. Stein. Asymptotic Behavior of the Stock Price Distribution Density and Implied Volatility in Stochastic Volatility Models, Applied Mathematics & Optimization, Volume 61, Number 3, 287-315, DOI: 10.1007/s00245-009-9085-x

[23] Patrick Hagan, Andrew Lesniewski, and Diana Woodward; Probability Distribution in the SABR Model of Stochastic Volatility. Working Paper 2005. Available on lesniewski.us/working.html

[24] Henry-Labordère P, Analysis, geometry and modeling in finance, Chapman and Hill/CRC, 2008.

[25] Heston S. 1993. A closed-form solution for options with stochastic volatility, with application to bond and currency options. Review of Financial Studies 6, 327–343.

[26] Shigeo Kusuoka and Yasufumi Osajima: A remark on the asymptotic expansion of density function of Wiener functionals. UTMS Preprint 2007-18.

[27] Roger Lee. The Moment Formula for Implied Volatility at Extreme Strikes, Mathematical Finance, vol 14 issue 3 (July 2004), 469-480.

[28] P.L. Lions and M. Musiela. Correlations and bounds for stochastic volatility models. *Ann. I.H. Poincaré*, 24, 2007, 1-16.

[29] Alex Lipton and Artur Sepp, Stochastic volatility models and Kelvin waves. 2008, *J. Phys. A: Math. Theor. 41*.

[30] S A Molchanov, "Diffusion processes and Riemannian geometry", Russ. Math. Surv., 1975, 30 (1), 1–63.

[31] R. Montgomery. A Tour of SubRiemannian Geometries, their Geodesics and Applications, Volume 91 of Mathematical Surveys and Monographs. American Mathematical Society, Providence, RI, 2002.

[32] Osajima, Yasufumi, General Asymptotics of Wiener Functionals and Application to Mathematical Finance (July 25, 2007). Available at SSRN: http://ssrn.com/abstract=1019587

[33] Huyen Pham, Large deviations in Finance, 2010, Third SMAI European Summer School in Financial Mathematics.

[34] V. Piterbarg, Markovian projection method for volatility calibration; RISK (2007).

[35] Sakai, T.: Riemannian Geometry, AMS, 1992.

[36] Seierstad, A. and Sydsaeter, K.: Optimal Control Theory with Economic Applications. (Advanced Textbooks in Economics, 24). North- Holland Amsterdam, 1987

[37] Stein, E. M., and J. C. Stein, 1991, “Stock Price Distributions with Stochastic Volatility: An Analytic Approach,” Review of Financial Studies, 4, 727-752.

[38] Varadhan, S. R. S., On the behavior of the fundamental solution of the heat equation with variable coefficients. Communications on Pure and Applied Mathematics, 20: 431–455. 1967